

## Modeling and simulation of chemically amplified electron beam, x-ray, and EUV resist processes

Takahiro Kozawa, Akinori Saeki, and Seiichi Tagawa

Citation: *Journal of Vacuum Science & Technology B* **22**, 3489 (2004); doi: 10.1116/1.1823435

View online: <http://dx.doi.org/10.1116/1.1823435>

View Table of Contents: <http://scitation.aip.org/content/avs/journal/jvstb/22/6?ver=pdfcov>

Published by the AVS: Science & Technology of Materials, Interfaces, and Processing

### Articles you may be interested in

Dependence of acid generation efficiency on the protection ratio of hydroxyl groups in chemically amplified electron beam, x-ray and EUV resists

*J. Vac. Sci. Technol. B* **22**, 3522 (2004); 10.1116/1.1813452

Correlation of atomic force microscopy sidewall roughness measurements with scanning electron microscopy line-edge roughness measurements on chemically amplified resists exposed by x-ray lithography

*J. Vac. Sci. Technol. B* **17**, 2723 (1999); 10.1116/1.591053

Extreme ultraviolet and x-ray resist: Comparison study

*J. Vac. Sci. Technol. B* **17**, 3379 (1999); 10.1116/1.591014

Comparative evaluation of electron-beam sensitive single layer top surface imaging and bilayer chemical amplification of resist lines process for stencil mask making

*J. Vac. Sci. Technol. B* **17**, 3122 (1999); 10.1116/1.590965

Radiation-induced reactions of chemically amplified x-ray and electron-beam resists based on deprotection of t-butoxycarbonyl groups

*J. Vac. Sci. Technol. B* **15**, 2582 (1997); 10.1116/1.589689


**SHIMADZU** Powerful, Multi-functional UV-Vis-NIR and FTIR Spectrophotometers

Excellence in Science

Providing the utmost in sensitivity, accuracy and resolution for applications in materials characterization and nano research

- Photovoltaics
- Polymers
- Thin films
- Paints
- Ceramics
- DNA film structures
- Coatings
- Packaging materials



[Click here to learn more](#)

# Modeling and simulation of chemically amplified electron beam, x-ray, and EUV resist processes

Takahiro Kozawa,<sup>a)</sup> Akinori Saeki, and Seiichi Tagawa<sup>b)</sup>

*The Institute of Scientific and Industrial Research, Osaka University, 8-1 Mihogaoka, Ibaraki, Osaka 567-0047, Japan*

(Received 3 June 2004; accepted 4 October 2004; published 15 December 2004)

With the shrinkage of feature sizes, ever precise accuracy has been required for process simulators because of the importance of nanoscale resist topography such as line edge roughness. Formation processes of latent images in chemically amplified electron beam (EB), x-ray, and EUV resists are different from both chemically amplified photoresists used in optical lithography and conventional, nonchemically amplified EB resists. A new simulation scheme precisely based on reaction mechanisms is necessary to reproduce resist patterns for the postoptical lithographies. We proposed a method to simulate electron dynamics in chemically amplified resists and to calculate the acid distribution around an ionization point with a typical parameter set. © 2004 American Vacuum Society. [DOI: 10.1116/1.1823435]

## I. INTRODUCTION

Modeling and simulation of resist processes have been important for the prediction of resist patterns. Many simulation models and methods have been developed. Especially, the interaction of an electron beam (EB) with resist materials (primary and secondary electron scattering),<sup>1-4</sup> the acid diffusion during PEB,<sup>5,6</sup> and development processes<sup>7-9</sup> have been well studied. These studies cover almost all the processes of resist pattern formation except for acid generation from the decomposition of the acid generators. As feature sizes get smaller, acid distribution at the molecular level becomes more important for resist pattern formation. The acid generation processes are key to understanding resist features below 65 nm such as line edge roughness and resolution limits.

The reaction mechanism at the molecular level must be taken into account for the reproduction of nanoscale resist topography. Two main channels leading to acid generation have been reported. One starts with the excitation of the acid generator<sup>10,11</sup> or the base polymer<sup>12,13</sup> (excitation channel). In some cases, acids are generated through the electron transfer from the excited state of the base polymer to the acid generator. The other starts with the ionization of the base polymer (ionization channel) as follows:<sup>14</sup>



where RH, RH<sup>+</sup>, e<sup>-</sup>, AG, A, G<sup>-</sup>, and HG are base polymer, its radical cation, an electron, an acid generator, its decomposed

fragment, a counter anion, and an acid. In photolithography such as KrF excimer lithography, the excitation channel dominates the acid generation processes. On the other hand, in EB lithography, the ionization channel dominates.<sup>15</sup> The ionization process is also likely to play an important role in the acid generation processes of EUV resists, because the energy of EUV is 92.5 eV. The acid generation processes of postoptical lithographies are entirely different from those of optical lithographies. Also, the formation processes of latent images in chemically amplified resists are different from those of conventional, nonchemically amplified EB resists such as poly(methylmethacrylate) (PMMA). For example, electrons with the energy less than 5 eV do not play any major role in the pattern formation processes of PMMA.<sup>16</sup> However, the dynamics of low energy electrons are essential to the formation of latent images in chemically amplified resists. Therefore, a simulation scheme for PMMA cannot be directly applied to chemically amplified resists.

In this paper, we proposed a simulation method to reproduce the acid distribution in chemically amplified EB, x-ray, and EUV resists and calculated the acid distribution around an ionization point with a typical parameter set.

## II. SIMULATION METHOD

For the formation of latent images in chemically amplified EB, x-ray, and EUV resists, low energy electrons (near thermal energy) play an important role in the acid generation processes.<sup>17</sup> The dynamics of low energy electrons can be described with the Smoluchowski equation,

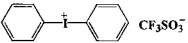
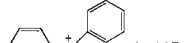
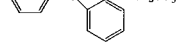
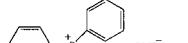
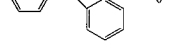
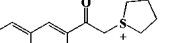
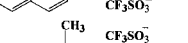
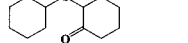
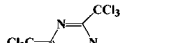
$$\frac{\partial w}{\partial t} = D_1 \nabla \left( \nabla w + w \frac{1}{k_B T} \nabla V \right), \quad (5)$$

where  $w$ ,  $D_1$ ,  $k_B$ ,  $T$ , and  $V$  represent the probability density of electrons, the mutual diffusion constant between an electron and a cation, the Boltzmann constant, the absolute temperature, and the Coulomb potential, respectively. The reaction of

<sup>a)</sup>Electronic mail: kozawa@sanken.osaka-u.ac.jp

<sup>b)</sup>Electronic mail: tagawa@sanken.osaka-u.ac.jp

TABLE I. Effective reaction radii of acid generators,  $R$ , and rate constants of reactions of acid generators with solvated electrons in methanol,  $k$ . The effective reaction radii of acid generators were roughly estimated from the rate constants under the assumption that the diffusion of acid generators is negligible. (These values are slightly overestimated because of this assumption.)

Acid generator	$k$ ( $M^{-1}s^{-1}$ )	$R$ (nm)
	$2.4 \times 10^{10}$	2.1
	$2.7 \times 10^{10}$	2.4
	$2.5 \times 10^{10}$	2.2
	$1.9 \times 10^{10}$	1.7
	$1.6 \times 10^{10}$	1.4
	$2.2 \times 10^{10}$	1.9
	$2.5 \times 10^{10}$	2.2
	$1.1 \times 10^{10}$	0.96
	$2.2 \times 10^{10}$	1.9

acid generators with electrons can be described with a pseudo-first-order reaction,

$$\frac{\partial w}{\partial t} = -kCw, \quad (6)$$

where  $k$  and  $C$  are the rate constant and the concentration of acid generators, respectively. However, the rate constants have been obtained only in solutions.<sup>14,18</sup> They cannot be applied directly to solid resist films, mainly because the diffusion constants of intermediates are different in each condition. In order to solve this problem, we propose the following procedure. The reaction of acid generators with electrons is controlled by electron diffusion.<sup>14</sup> In such case, the rate constant for counter anion generation can be described as follows:

$$k = 4\pi RD_2, \quad (7)$$

where  $R$  and  $D_2$  are an effective reaction radius of the acid generator and the mutual diffusion constant between an electron and an acid generator, respectively. The rate constants of acid generators with electrons have been determined using solvated electrons in methanol as listed in Table I.<sup>18</sup> These

values were obtained using a pulse radiolysis method. The mobility of solvated electrons in methanol was reported to be  $0.00059 \text{ cm}^2 \text{ V}^{-1} \text{ s}^{-1}$ .<sup>19</sup> Therefore, the effective reaction radii of acid generators can be roughly estimated under the assumption that the diffusion of acid generators is negligible compared to solvated electrons. These values are slightly overestimated because of this assumption.

Assumed that electron mobility is much higher than those of other species, the dynamics of acid generation in real chemically amplified resists can be described as follows:

$$\frac{\partial w}{\partial D_e t} = \nabla \left( \nabla w + w \frac{1}{k_B T} \nabla V \right) - 4\pi RCw, \quad (8)$$

where  $D_e$  is the diffusion constant of electrons. After the application of spherical symmetry, Eq. (8) becomes

$$\frac{\partial w}{\partial D_e t} = \left( \frac{\partial^2 w}{\partial r^2} + \left( \frac{2}{r} + \frac{e^2}{4\pi\epsilon_0\epsilon_k B T r^2} \right) \frac{\partial w}{\partial r} \right) - 4\pi RCw, \quad (9)$$

where  $e$ ,  $\epsilon_0$ , and  $\epsilon$  are elementary electric charge, dielectric constant in vacuum and relative dielectric constant of resist films, respectively.

It was reported that the temporal change of separation distance between electrons (anion sources) and radical cations (proton sources) can be obtained by the analysis of time-dependent behaviors of geminate ion pairs,<sup>20</sup> which were observed using a subpicosecond pulse radiolysis method.<sup>21</sup> In the previous investigations, *n*-dodecane and benzene were used as model compounds of base polymers and the spatiotemporal dynamics of low energy electrons were reproduced. The initial separation distances in *n*-dodecane and benzene were 6.6 and 3.2 nm, respectively.<sup>20,22</sup> In both compounds, an exponential distribution function as an initial distribution was reported to well reproduce the following time-dependent behavior of intermediates:

$$w_{t=0} r^2 dr = \frac{1}{r_0} \exp\left(-\frac{r}{r_0}\right) dr, \quad (10)$$

where  $r_0$  is an initial separation distance on average between a thermalized electron and its parent radical cation. The initial separation distance in aromatic polymers is likely to be longer than one in benzene and shorter than one in *n*-dodecane.<sup>17</sup> Although a precise initial separation distance is unknown, a value between 3.2 and 6.6 nm is considered to give a good approximation.

### III. RESULTS AND DISCUSSION

The probability density of acid formation around an ionization point was calculated. Parameters were chosen to simulate a typical chemically amplified EB resist based on poly(4-hydroxystyrene) (PHS,  $C_8H_8O$ ) as follows: the initial separation distance,  $r_0=4$  nm, and the relative dielectric constant,  $\epsilon=4$ . Triphenylsulfonium–triflate was selected as an acid generator. The concentration and the effective reaction radius are 5 wt. % and 2.4 nm, respectively. Calculations were continued until the survival probability of electrons

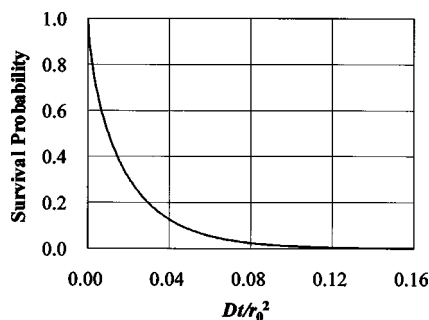


FIG. 1. Time profile of survival probability of electrons calculated with the parameters: the concentration of acid generator,  $C=5$  wt. %, the initial separation distance,  $r_0=4$  nm, the dielectric constant,  $\epsilon=4$ , the effective reaction radius,  $R=2.4$  nm.  $Dt/r_0^2$  is a nondimensional parameter and represents the elapsed time after the thermalization of electrons.

reached less than 0.1% of initial yield as shown in Fig. 1. The temporal changes of electron distribution were shown in Fig. 2. The vertical axis represents the probability density of electrons per unit spherical shell thickness. The horizontal axis represents a distance between a radical cation (ionization point) and an electron. The radical cation is located at the origin. The probability density was normalized so that the integration of initial distribution is equal to 1. The electrons near the origin rapidly recombine with their parent radical cations due to the strong electric field produced by radical cations. Counter anions are produced via dissociative electron attachment of acid generators. The evolution of the counter anion distribution is shown in Fig. 3. The distribution of probability density of counter anions in the  $x$ - $y$  plane is shown in Fig. 4. Counter anions are distributed around the ionization point according to the probability shown in Fig. 4. Although the probability density has a maximum around the ionization point, the highest density was  $0.05 \text{ nm}^{-3}$ . The average distance between anions and the ionization point was 6.0 nm. Protons are generated near the ionization point via deprotonation of radical cations of base polymers. The deprotonation efficiencies depend on polymer structure.<sup>23</sup> It was reported that the radical cations of PHS produce protons nearly at 100% efficiency if they can escape the recombination reaction with electrons.<sup>24</sup> In this simulation, the escape

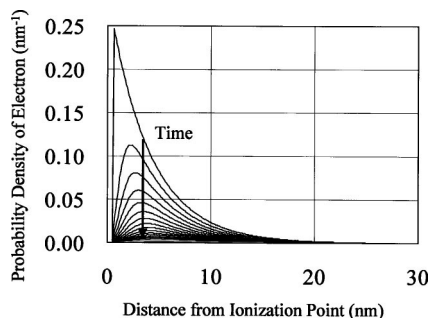


FIG. 2. Distribution change of electrons around an ionization point. The vertical axis represents the probability density of electrons per unit spherical shell thickness. The time step ( $\Delta Dt/r_0^2$ ) between each line is 0.005 and the maximum time ( $Dt/r_0^2$ ) is 0.16.

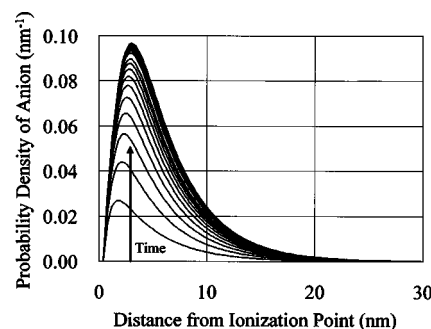


FIG. 3. Evolution of counter anion distribution. The vertical axis represents the counter anion probability density per unit spherical shell thickness. The time step ( $\Delta Dt/r_0^2$ ) between each line is 0.005 and the maximum time ( $Dt/r_0^2$ ) is 0.16.

probability was 0.68. However, the protection of hydroxyl groups of PHS affects deprotonation efficiencies. The efficiencies depend on the type of protecting groups. Some of them have been reported.<sup>25-27</sup> Protons will be generated according to the deprotonation efficiencies of base polymers. This means that even if a base polymer is ionized by exposure and a counter anion is generated by the reaction of an acid generator with an electron, an acid may not be generated. Acid distribution has been considered uniform in chemically amplified resists. However, as feature sizes get close to the distance between acids generated by exposure,<sup>24</sup> the inhomogeneous acid distribution caused by the difference of deprotonation efficiencies among monomer units is considered to have greater impact on the resist topography. After protons are detached from base polymers, they migrate in a resist matrix. It has been proved that protons can move in PHS (Ref. 24) and PMMA matrices<sup>28</sup> even at room temperature. The dynamics of protons can be also described by Eq. (5). The reaction of electrons with acid generators or parent radical cation is so fast<sup>17</sup> that we can treat each cation-electron pair independently. However, protons move much slower than electrons.<sup>28</sup> Therefore, the dynamics of the proton-anion pair are affected by other ions which are accumulated during exposure. To precisely reproduce the acid distribution, we have to solve a many body problem according to Eq. (5). This is a time consuming task. However, it is well known that acids hardly migrate in resist matrices at

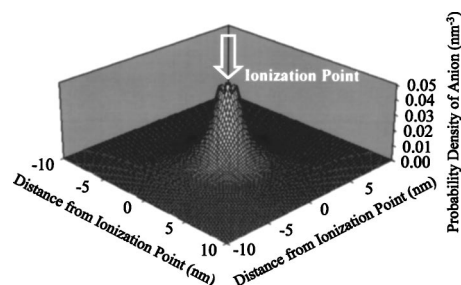


FIG. 4. Distribution of probability density of counter anions in the  $x$ - $y$  plane after the survival probability of electrons reached less than 0.1% of initial yield. The coordinate of ionization point is the origin. Proton generation efficiency at the ionization point depends on the polymer structure.



room temperature.<sup>29,30</sup> This is because counter anions of acids cannot move. Especially, bulky anions used in recent resist formula are unlikely to move at room temperature. Therefore, protons are likely to move toward counter anions. Assuming that counter anions are fixed where they are produced, the acid probability density is considered approximately same as counter anion distribution. Although electrons with the energy less than 5 eV do not play any major role in the pattern formation processes of PMMA, the low energy electrons determine the acid distribution, and consequently the resist pattern, in chemically amplified resists.

#### IV. CONCLUSION

Many simulation models and methods have been developed. However, modeling of acid generation processes induced by ionizing radiation has not been reported. The formation processes of latent images of EB, x-ray, and EUV resists are different from those of both chemically amplified photoresists and conventional EB resists. The acid generation processes are a key to understanding and reproducing the resist pattern formation. We proposed a new simulation scheme for chemically amplified EB, x-ray, and EUV resists based on their reaction mechanism. This scheme is applicable to exposure sources which have higher energy than the ionization potential of the resist materials. We simulated the acid formation processes in PHS-based chemically amplified resists and calculated the distribution of acid probability density around an ionization point. The average distance between acids and the ionization point was 6.0 nm. This blur is not negligible in the viewpoint of nanofabrication below the 65 nm node.

<sup>1</sup>R. J. Hawryluk, A. M. Hawryluk, and H. I. Smith, *J. Appl. Phys.* **45**, 2551 (1974).

<sup>2</sup>R. Shimizu, T. Ikuta, T. E. Everhart, and W. J. DeVore, *J. Appl. Phys.* **46**, 1581 (1975).

<sup>3</sup>D. F. Kyser, *J. Vac. Sci. Technol. B* **1**, 1391 (1983).

<sup>4</sup>G. Han, M. Khan, Y. Fang, and F. Cerrina, *J. Vac. Sci. Technol. B* **20**, 2666 (2002).

<sup>5</sup>J. Nakamura, H. Ban, K. Deguchi, and A. Tanaka, *Jpn. J. Appl. Phys.*,

Part 1 **30**, 2619 (1991).

<sup>6</sup>K. Nakazawa and M. Sasago, *Jpn. J. Appl. Phys.*, Part 1 **39**, 1944 (2000).

<sup>7</sup>C. A. Mack, *J. Electrochem. Soc.* **134**, 148 (1987).

<sup>8</sup>C. A. Mack and G. Arthur, *Electrochem. Solid-State Lett.* **1**, 86 (1998).

<sup>9</sup>A. R. Neureuther, D. F. Kyser, and C. H. Ting, *IEEE Trans. Electron Devices* **26**, 686 (1979).

<sup>10</sup>S. P. Pappas, B. C. Pappas, and L. R. Gatechair, *J. Polym. Sci., Polym. Chem. Ed.* **22**, 69 (1984).

<sup>11</sup>J. L. Dektar and N. P. Hacker, *J. Org. Chem.* **55**, 639 (1990).

<sup>12</sup>N. P. Hacker, D. C. Hofer, and K. M. Welsh, *J. Photopolym. Sci. Technol.* **5**, 35 (1992).

<sup>13</sup>J. F. Cameron, N. Chan, K. Moore, and G. Pohlers, *Proc. SPIE* **4345**, 106 (2001).

<sup>14</sup>T. Kozawa, Y. Yoshida, M. Uesaka, and S. Tagawa, *Jpn. J. Appl. Phys.*, Part 1 **31**, 4301 (1992).

<sup>15</sup>S. Tagawa, S. Nagahara, T. Iwamoto, M. Wakita, T. Kozawa, Y. Yamamoto, D. Werst, and A. D. Trifunac, *Proc. SPIE* **3999**, 204 (2000).

<sup>16</sup>A. N. Broers, *IBM J. Res. Dev.* **32**, 502 (1988).

<sup>17</sup>T. Kozawa, A. Saeki, A. Nakano, Y. Yoshida, and S. Tagawa, *J. Vac. Sci. Technol. B* **21**, 3149 (2003).

<sup>18</sup>S. Tsuji, T. Kozawa, Y. Yamamoto, and S. Tagawa, *J. Photopolym. Sci. Technol.* **13**, 733 (2000).

<sup>19</sup>P. Fowles, *Trans. Faraday Soc.* **67**, 428 (1971).

<sup>20</sup>A. Saeki, T. Kozawa, Y. Yoshida, and S. Tagawa, *Jpn. J. Appl. Phys.*, Part 1 **41**, 4213 (2002).

<sup>21</sup>T. Kozawa, A. Saeki, Y. Yoshida, and S. Tagawa, *Jpn. J. Appl. Phys.*, Part 1 **41**, 4208 (2002).

<sup>22</sup>K. Okamoto, A. Saeki, T. Kozawa, Y. Yoshida, and S. Tagawa, *Chem. Lett.* **32**, 834 (2003).

<sup>23</sup>H. Yamamoto, T. Kozawa, A. Nakano, K. Okamoto, and S. Tagawa, *Jpn. J. Appl. Phys.*, Part 1 **43**, 3971 (2004).

<sup>24</sup>H. Yamamoto, T. Kozawa, A. Nakano, K. Okamoto, Y. Yamamoto, T. Ando, M. Sato, H. Komano, and S. Tagawa, *Jpn. J. Appl. Phys.*, Part 2 **43**, L848 (2004).

<sup>25</sup>H. Yamamoto, T. Kozawa, A. Nakano, K. Okamoto, Y. Yamamoto, S. Tagawa, T. Ando, M. Sato, and H. Komano, *J. Vac. Sci. Technol. B*, these proceedings.

<sup>26</sup>T. Kozawa, S. Nagahara, Y. Yoshida, and S. Tagawa, *J. Vac. Sci. Technol. B* **15**, 2582 (1997).

<sup>27</sup>A. Nakano, K. Okamoto, T. Kozawa, and S. Tagawa, *Jpn. J. Appl. Phys.*, Part 1 **43**, 3981 (2004).

<sup>28</sup>A. Nakano, K. Okamoto, T. Kozawa, and S. Tagawa, *Jpn. J. Appl. Phys.*, Part 1 **43**, 4363 (2004).

<sup>29</sup>H. Fedynyshyn, M. F. Cronin, and C. R. Szmanda, *J. Vac. Sci. Technol. B* **9**, 3380 (1991).

<sup>30</sup>S. V. Postnikov, M. D. Stewart, H. V. Tran, M. A. Nierode, D. R. Medeiros, T. Cao, J. Byers, S. E. Webber, and C. G. Wilson, *J. Vac. Sci. Technol. B* **17**, 3335 (1999).